The International Journal of Biochemistry & Cell Biology 81 (2016) 419–426

Contents lists available at ScienceDirect

The International Journal of Biochemistry & Cell Biology

journal homepage: www.elsevier.com/locate/biocel

Role of transition metals present in air particulate matter on lung oxygen metabolism

Natalia D. Magnani[a], Timoteo Marchini[a], Mariana Garcés[a], Andrea Mebert[b], Lourdes Cáceres[a], Luis Diaz[b], Martín Desimone[b], Pablo A. Evelson[a,*]

[a] Universidad de Buenos Aires, CONICET, Instituto de Bioquímica Medicina Molecular (IBIMOL), Cátedra de Química General e Inorgánica, Facultad de Farmacia y Bioquímica, Buenos Aires, Argentina
[b] Universidad de Buenos Aires, CONICET, Instituto de Química y Metabolismo del Fármaco (IQUIMEFA), Càtedra de Química Analítica Instrumental, Facultad de Farmacia y Bioquímica, Buenos Aires, Argentina

ARTICLE INFO

Article history:
Received 13 July 2016
Received in revised form 7 October 2016
Accepted 11 October 2016
Available online 14 October 2016

Keywords:
Air pollution
Lung
Transition metals
NADPH oxidase
Reactive O_2 species

ABSTRACT

Several epidemiological studies have shown a positive correlation between daily increases in airborne particulate matter (PM) concentration and the occurrence of respiratory and cardiovascular diseases. Transition metals present in air PM were associated with adverse health effects after PM exposure. The aim of this work was to study lung O_2 metabolism after an acute exposure to transition metal-coated nanoparticles (NPs). Female Swiss mice (25 g) were intranasally instilled with a suspension of silica NP containing Ni (II), Cd (II), Fe (III), or Cr (VI) at 0, 0.01, 0.05, 0.1, and 1.0 mg metal/kg body weight. Lung O_2 consumption was found to be significantly increased after the exposure to most doses of Ni-NP and Fe-NP, and the 0.05 mg metal/kg body weight dose of Cr-NP, while no changes were observed for Cd-NP. Lucigenin chemiluminescence (as an indicator of NADPH oxidase (NOX) activity) was evaluated in lung homogenates. Only Ni-NP and Fe-NP have shown the ability to induce a significant increase in lucigenin chemiluminescence. In order to establish the possible occurrence of pulmonary oxidative stress, TBARS levels and the GSH/GSSG ratio were determined. The higher doses of Ni-NP and Fe-NP were able to induce an oxidative stress condition, as shown by changes in both TBARS levels and the GSH/GSSG ratio. Taken together, the present results show differential effects for all the metals tested. These findings emphasize the importance of transition metals present air PM in PM adverse health effects, and contribute to the understanding of the pathological mechanisms triggered by the exposure to environmental PM.

1. Introduction

There is strong evidence that a short-term exposure to environmental air pollution particles currently represent a serious risk to human health (Dominici et al., 2006). Specifically, numerous epidemiological studies have shown a positive correlation between daily increases in airborne particulate matter (PM) concentration and the onset and aggravation of respiratory and cardiovascular diseases (Analitis et al., 2006).

Airborne PM consist of a heterogeneous mixture of solid particles emitted into the atmosphere from different natural and anthropogenic sources. PM suspended in air may vary in size, chemical composition, and sources of origin (Nel, 2005). PM size determine both their lifetime in the atmosphere and distribution within the lung. Biologically relevant particles comprise PM with an aerodynamic diameter below 10 μm, which are small enough to penetrate and deposit in the tracheobronchial tree (Brook et al., 2004). The smaller the particle the deeper it can penetrate into the airways and the higher diameter/surface area ratio, in which a larger number of potentially harmful chemicals could be absorbed and delivered up to the alveoli. For these reasons, nano-scale particles are a major concern regarding environmental PM toxicity (Delfino et al., 2005).

Fossil fuel combustion has been identified as one the major PM emission source, which mainly contribute to airborne PM burden with inorganic compounds. Recent studies have been conducted in order to establish associations between air pollution toxic mecha-

Abbreviations: NP, nanoparticles; PM, particulate matter; $O_2^{\bullet -}$, superoxide anion; NOX, NADPH oxidase; TBARS, thiobarbituric acid reactive substances; GSH, reduced glutathione; GSSG, oxidized glutathione.

* Corresponding author at: Universidad de Buenos Aires, CONICET, Instituto de Bioquímica y Medicina Molecular (IBIMOL), Catedra de Química General e Inorgánica, Facultad de Farmacia y Bioquímica, Junín 956 (1113), Buenos Aires, Argentina.
E-mail address: pevelson@ffyb.uba.ar (P.A. Evelson).

http://dx.doi.org/10.1016/j.biocel.2016.10.009
1357-2725/

nisms and specific PM components. Among the most frequent ones, transition metals within the fine PM fraction are of great toxicological interest (Leonard et al., 2004). The focus has often been on iron (Fe), vanadium (V), nickel (Ni), chromium (Cr), copper (Cu), cadmium (Cd) and zinc (Zn), on the basis of their ability to generate reactive oxygen species (ROS) in biological tissues and produce an oxidative stress condition (Chen and Lippmann, 2009). Consequently, one of the main suggested mechanisms of PM toxicity is the occurrence of pulmonary oxidative stress. Indeed, lung injury after air pollution PM inhalation has been shown to be triggered by local reactive O_2 species production that could be generated not only from the particles themselves, but also from the chemicals coated on their surface (Li and Nel, 2008). In line with this findings, previous results from our group using a PM surrogate with high transition metal content (Residual Oil Fly Ash, ROFA), showed an imbalance in pulmonary oxidative metabolism with a peak at 1 h after the instillation of the ROFA suspension (Magnani et al., 2011). In this scenario, the production of $O_2^{\bullet -}$ by the assembly and activation of the NADPH oxidase complex might play a central role (Magnani et al., 2013).

The relative contribution of transition metals in pulmonary physiopathological alterations is critical to understand PM toxicity. Some effects of PM-associated transition metals have already been described. However, the classical experimental approach in such studies has been the delivery of metal ions solutions or the use of particles deprived from transition metals by washing or chelation (Chen and Lippmann, 2009). Therefore, to better characterize their effect as PM components, we built silica nanoparticles (NPs) coated with single transition metals and evaluated lung O_2 metabolism in mice after an acute exposure.

2. Materials and methods

2.1. Silica NP preparation and characterization

Metal-coated silica NPs were prepared using the Stöber method (Stöber and Fink, 1968). Dense amorphous silica NP synthetized via base-catalyzed hydrolysis and polymerization of tetraethylorthosilicate were employed. It has been shown that the use of dense amorphous silica minimizes the biological effect of silica NP (Thomassen et al., 2010). Briefly, 12.5 mL of tetraethylorthosilicate (TEOS 98% w/w) was mixed with 50 mL ethanol. Afterwards, 5 mL ultrapure water and 4 mL NH_4OH (25% w/w) were added dropwise to the solution. In order to obtain NP coated with the different metal ions, 100 mg of $CdCl_2$, $K_2Cr_2O_7$, $Ni(NO_3)_2$, or $FeCl_3{\cdot}6H_2O$ were used as Cd(II), Cr(IV), Ni(II), or Fe(III) sources, respectively. The reaction mixture was kept at room temperature for 24 h with continuous stirring. The resulting metal-coated particles were centrifuged and washed three times with ethanol to remove ammonia, unreacted silica precursors, and soluble metal ions (Foglia et al., 2011). NP suspensions were freshly prepared by resuspending NP in sterile saline solution, followed by a 10 min incubation in an ultrasonic water bath before use (Goldsmith et al., 1998).

NP hydrodynamic diameter was measured by Dynamic Light Scattering (DLS) in a Zetasizer Nano-Zs equipment (Malvern Instruments, United Kingdom). A He-Ne laser (633 nm) and a ZEN3600 digital detector (Malvern Instruments) were used. Measurements were performed with a scatter angle of 173° and a fixed laser position of 4.65 mm at 25 °C. Results were expressed as nm (Kunzman et al., 2011).

NP size, morphology, and distribution were analyzed by Scanning Electron Microscopy (SEM) and Transmission Electron Microscope (TEM). A drop of the NP suspension was air dried onto a carbon film-coated grid. Afterwards, SEM was assessed in a Zeiss EVO 40 (Carl-Zeiss, Oberkochen, Germany) at 20000X and TEM was performed in a Zeiss EM 109T (Carl-Zeiss) at 12000X (Fischer et al., 1983).

NP metal content was evaluated by Atomic Absorption Spectrometry in a VGP 210 atomic absorption spectrometer (Buck Scientific, East Norwalk, CT, USA) by the electrothermal atomization method using pyrolytic graphite tubes. Each sample was injected in triplicate (Copello et al., 2007).

2.2. NP Fenton chemistry

In order to test NP ability to induce Fenton-like chemical reactions, the consumption of H_2O_2 generated by the glucose/glucose oxidase system by metal-coated NP was measured. H_2O_2 production rate was evaluated by the Amplex Red-horseradish peroxidase (HRP) method (Chen et al., 2003). After an initial stabilization period, 1 mM glucose and 1 ng/mL glucose oxidase were added to the reaction mixture. Resorfurin formation due to Amplex Red (25 μM) oxidation by HRP (0.5 U/mL) bound to H_2O_2 was measured in Perkin Elmer LS 55 Fluorescence Spectrometer (Perkin Elmer, Waltham, MA, USA) at 563 nm (excitation) and 587 nm (emission). Afterwards, 50 μg/mL of silica NP or metal-coated NP (Cd-NP, Cr-NP, Ni-NP, Fe-NP) suspensions were added. A calibration curve was performed using H_2O_2 solutions as standard and H_2O_2 production rate was expressed as pmol/min.

2.3. Animal model of exposure to NP

Female Swiss mice weighing 20–25 g were exposed to NP by the nasal drop technique as previously described (Southam et al., 2002). Briefly, mice were randomized, lightly anaesthetized (i.p.) with 1 mL/kg body weight of xylazine (2% w/v) and ketamine (50 mg/mL), and intranasally instilled with 50 μL of the NP suspension (0.01 to 1.0 mg metal/kg body weight) delivered in a single dose. Control mice were handled in parallel and instilled with 50 μL of an empty silica NP suspension or saline solution (vehicle). The metal doses were selected based on results shown in previous studies (Arantes-Costa et al., 2008; Magnani et al., 2011 and 2013). Animals were sacrificed 1 h after NP exposure with an anesthesia overdose and lung samples were collected. Animal treatment was carried out in accordance with the guidelines of the 6344/96 regulation of the Argentinean National Drug, Food and Medical Technology Administration (ANMAT).

2.4. Samples preparation

2.4.1. Tissue cubes

Once the exposure time was reached, animals were sacrificed and lungs were removed and immediately placed in ice-cold Krebs buffer solution. After being washed and weighted, 1 mm^3 tissue cubes were cut by the use of a scalpel (Vanasco et al., 2008).

2.4.2. Tissue homogenates

Lung samples (0.2 g of wet weight) were homogenized with a glass-Teflon homogenizer in a medium consisting of 120 mM KCl, 30 mM phosphate buffer (pH 7.4) (1:5) at 0–4 °C. The suspension was centrifuged at 600*g* for 10 min at 4 °C to remove nuclei and cell debris. The pellet was discarded and the supernatant was used as "homogenate" (Evelson et al., 2001). Protein concentration was measured by the method of Lowry et al. (1951) using BSA as standard.

2.5. Oxygen consumption by tissue cubes

A two-channel respirometer for high-resolution respirometry (Hansatech Oxygraph, Hansatech Instruments Ltd., Norfolk, England) was used. O_2 consumption rates were measured at 30 °C in a

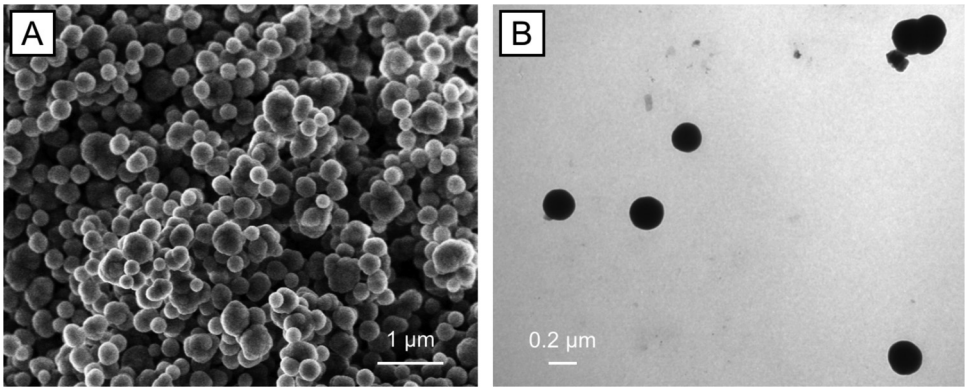

Fig. 1. NPs characterization. A) Silica NP Scanning Electronic Microscopy at 20000×, scale bar 1 μm. B) Silica NP Transmission Electronic Microscopy at 12000×, scale bar 0.5 μm.

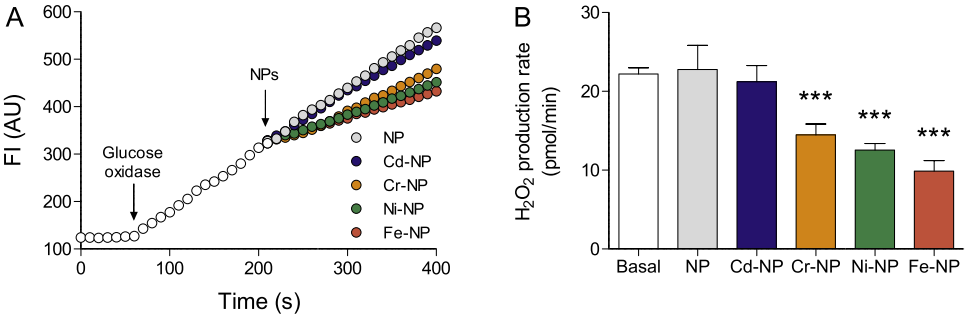

Fig. 2. NPs Fenton chemistry. A) Inhibition of H_2O_2 production by the glucose–glucose oxidase system using empty silica NPs (50 μg/mL) or metal-coated NPs (Cd-NP, Cr-NP, Ni-NP, Fe-NP) suspensions (50 μg/mL). B) H_2O_2 production rates were calculated from the slopes in A) and a calibration curve using H_2O_2 solutions as standard. ***$p < 0.001$ vs. basal H_2O_2 production rate.

Krebs buffer (Poderoso et al., 1994). KCN (4 mM) was added to the reaction chamber as a mitochondrial cytochrome oxidase inhibitor (Vanasco et al., 2008). Results were expressed as ng-at O/min g tissue.

2.6. Lucigenin chemiluminescence for superoxide and superoxide-products

The lucigenin-derived chemiluminescence method was used as an indirect measurement of Nox activity (Vaquero et al., 2004). Briefly, 50 μg of protein tissue homogenate was diluted in 250 μL of 50 mM phosphate buffer containing 1 mM EGTA and 150 mM sucrose (pH 7.4). Lucigenin (50 μM) was added to the reaction media, 100 μM NADPH was used as substrate, and chemiluminescence was immediately measured at 15 s intervals for 3 min in a Labsystems Luminoskan RS Microplate Reader (Labsystem, Ramsey, MN, USA). The specificity of the assay was confirmed by the addition of superoxide dismutase (200 U/mL) as an $O_2^{\bullet -}$ scavenger. Results were expressed in arbitrary units (AU)/mg protein.

2.7. Thiobarbituric acid reactive substances (TBARS) assay

Oxidative damage to phospholipids was evaluated as TBARS by a fluorometric assay (Yagi, 1976). Briefly, 100 μL of lung homogenates were added to 200 μL 0.1 N HCl, 30 μL 10% (w/v) phosphotungstic acid, and 100 μL 0.7% (w/v) 2-thiobarbituric acid. The mixture was heated in boiling water for 60 min. TBARS were extracted in *n*-butanol. After a centrifugation at 1000*g* for 10 min, the fluorescence of the butanolic layer was measured in a LS 55 Fluorescence Spectrometrer (Perkin Elmer) at 515 nm (excitation) and 553 nm (emission). A calibration curve was prepared using 1,1,3,3-tetramethoxypropane as standard. Results were expressed as pmol TBARS/mg protein.

2.8. Reduced (GSH) and oxidized (GSSG) glutathione levels

Lung samples were homogenized with a glass-Teflon homogenizer in solution containing 1 M $HClO_4$–2 mM EDTA (1:1), and centrifuged at 16000*g* for 20 min at 4 °C. Supernatants were filtered through 0.22 μm cellulose acetate membranes (Corning Inc., NY, USA) and frozen at −80 °C until use. HPLC analysis was performed in a Perkin Elmer LC 250 liquid chromatograph, equipped with a Perkin Elmer LC ISS 200 advanced sample processor, and a Coulochem II (ESA, Bedford, MA, USA) electrochemical detector. A Supelcosil LC-18 (250 × 4.6 mm ID, 5 μm) column protected by a Supelguard (20 × 4.6 mm ID) precolumn (Supelco, Bellfonte, PA, USA) was used for sample separation. GSH and GSSG were eluted at a flow rate of 1.2 mL/min with 20 mM sodium phosphate (pH 2.7), and electrochemically detected at an applied oxidation potential of +0.800 V. Results were expressed as μM (Rodriguez-Ariza et al., 1994).

2.9. Drugs and chemicals

All chemicals were purchased from Sigma-Aldrich Chemical Company (St. Louis, MO, USA), except from HCl, H_2SO_4, and organic solvents which were purchased from Merck KGaA (Darmstadt, Germany).

2.10. Statistics

Results were expressed as mean values ± SEM and represent the mean of at least 6 independent experiments. Each indepen-

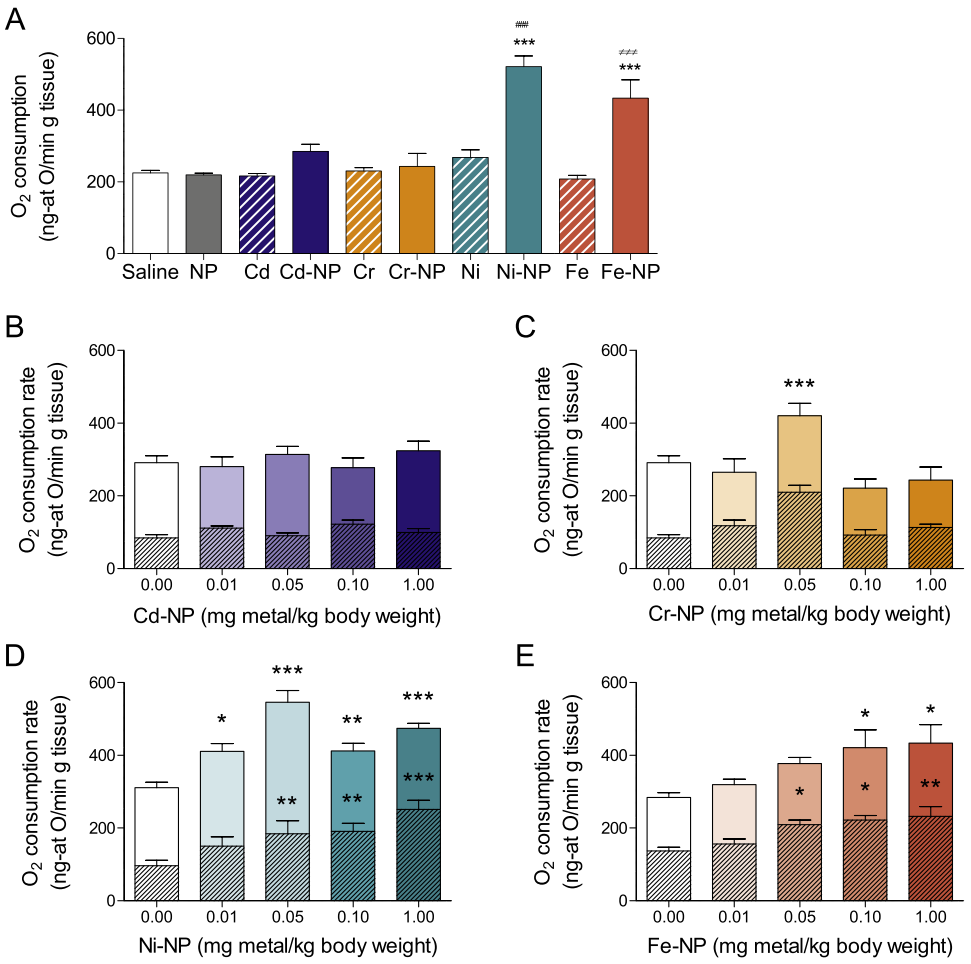

Fig. 3. Lung O_2 metabolism after the exposure to metal-coated NPs. A) Lung O_2 consumption was evaluated after intranasal instillation with saline, empty silica NPs, metal ions (Cd(II), Cr(VI), Ni(II), Fe(III); hatched bars) solutions (1.0 mg metal/kg body weight), or metal-coated NPs (Cd-NP, Cr-NP, Ni-NP, Fe-NP; flat bars) suspensions (1.0 mg metal/kg body weight). $^{***}p < 0.001$ vs. NP; $^{\#\#\#}p < 0.001$ vs. Ni; and $^{\neq\neq\neq}p < 0.001$ vs. Fe. Tissue O_2 consumption was also evaluated in lung samples from mice exposed to increasing doses of B) Cd-NP, **C**) Cr-NP, D) Ni-NP, or E) Fe-NP. Flat bars in B-E represent total lung O_2 consumption while hatched bars indicate O_2 consumption in the presence of KCN 4 mM $^{*}p < 0.05$, $^{**}p < 0.01$, and $^{***}p < 0.001$ vs. the corresponding control group for each metal (0 mg metal/kg body weight).

Table 1
NPs characterization. Silica and metal-coated NP size was measured as aerodynamic diameter by Dynamic Light Scattering and metal content was analyzed by Atomic Absorption Spectroscopy.

	Aerodynamic diameter (nm)	Metal content (mg metal/g NP)
NP	170 ± 2	nd
Cd-NP	550 ± 70	9.1 ± 0.4
Cr-NP	690 ± 20	18.0 ± 0.9
Ni-NP	200 ± 20	22.3 ± 0.2
Fe-NP	600 ± 50	1.0 ± 0.2

dent sample was also measured by duplicate. Unpaired Student's *t*-test was used to analyze differences between two groups. ANOVA followed by the Student-Newman-Keuls test was performed to analyze differences between more than two groups. Statistical significance was considered at $p < 0.05$.

3. Results

3.1. NP characterization

Metal-coated NP morphology was studied by TEM and SEM (Fig. 1). NP size and metal content were also evaluated and results are shown in Table 1. According to their aerodynamic diameter, every constructed NP represents fine (aerodynamic diameter < 2.5 μm) and ultrafine (aerodynamic diameter < 0.1 μm) air PM fractions.

3.2. NP Fenton-like chemistry

Consumption of H_2O_2 produced by the glucose/glucose oxidase system due to the addition of metal-coated NPs (Fig. 2A) was used as an index of their ability to participate in Fenton-like chemical reactions. As it is shown in Fig. 2B, Cr-NP, Ni-NP, and Fe-NP were able to significantly decrease H_2O_2 production, indicating that they are able to induce the production of reactive O_2 species by Fenton-like chemical reactions.

3.3. Tissue O_2 consumption

To evaluate O_2 metabolism by the whole tissue, respiration rates were assessed in 1 mm^3 lung tissue cubes, a thickness that allows O_2 diffusion to the center of the cube avoiding anaerobic areas (Valdez et al., 2011). As a first approach, O_2 consumption after empty silica NP exposure was compared with that from mice instilled with saline solution, which was used as the vehicle in every metal-coated NP suspension. No significant differences were observed between both groups (Fig. 3A), indicating that silica NP *per se* does not affect lung O_2 metabolism in our model. The effects

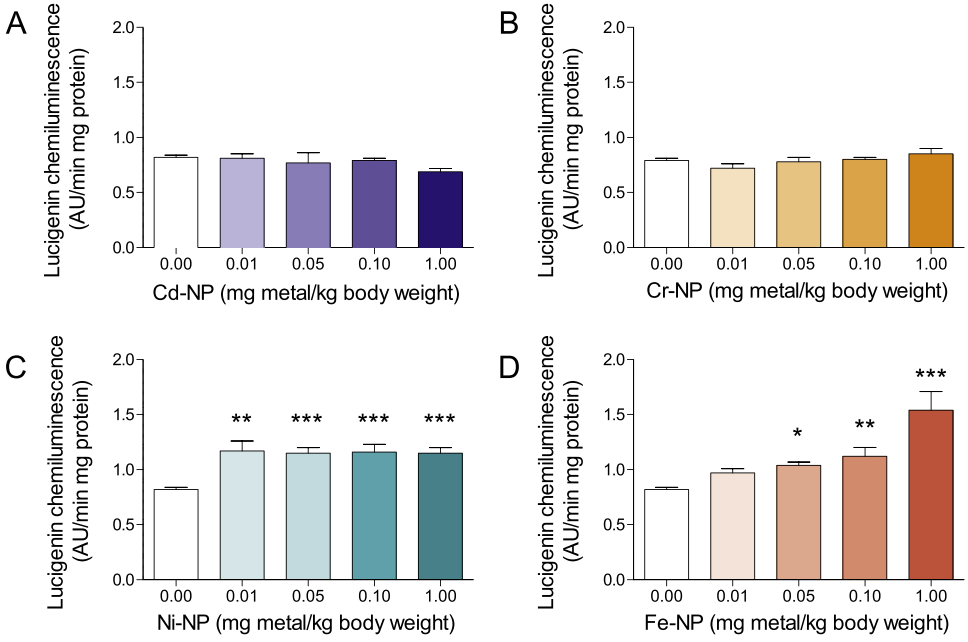

Fig. 4. Lucigenin chemiluminescence for superoxide and superoxide products in lung homogenates after the exposure to metal-coated NPs. NOX activity was evaluated by lucigenin chemiluminescence induced by NADPH-dependent $O_2^{\bullet-}$ production in lung homogenates from mice exposed to increasing doses of A) Cd-NP, B) Cr-NP, C) Ni-NP, or D) Fe-NP. $^{*}p < 0.05$, $^{**}p < 0.01$, and $^{***}p < 0.001$ vs. the corresponding control group for each metal (0 mg metal/kg body weight).

triggered by each metal ion delivered as a metal solution was also compared with the administration of an equivalent amount of metal but present in their respective metal-coated NP, to reach the higher dose at 1 mg metal/kg body weight. Mice exposed to Ni-NP and Fe-NP showed a significant increase in O_2 consumption rate when compared, not only with the empty silica NP group ($p < 0.01$), but also with Ni(II) or Fe(III) ions solutions exposure, respectively ($p < 0.01$) (Fig. 3A).

Total tissue O_2 consumption was also assessed in lung samples from every metal-coated NP experimental group, using increasing metal doses. To distinguish total O_2 uptake and that from non-mitochondrial sources, measurements were also performed in the presence of KCN, as a mitochondrial cytochrome oxidase inhibitor. After Cd-NP exposure, no differences were observed in any experimental group when compared with the control, neither for total O_2 consumption (0 mg metal/kg body weight: 291 ± 20 ng-at O/min g tissue) nor for non-mitochondrial O_2 consumption (0 mg metal/kg body weight: 84 ± 9 ng-at O/min g tissue) (Fig. 3B). As it is shown in Fig. 3C, Cr-NP administration induced a significant increase by 45% in total O_2 consumption at 0.05 mg metal/kg body weight ($p < 0.001$), while no differences where observed in the rest of the doses compared to the control group (0 mg metal/kg body weight: 290 ± 20 ng-at O/min g tissue). Lung O_2 consumption in the presence of KCN showed the same pattern as the described for total O_2 consumption, a significant increase by 50% at 0.05 mg metal/kg body weight (0 mg metal/kg body weight: 84 ± 9 ng-at O/min g tissue, $p < 0.001$) (Fig. 3C). When total O_2 consumption was evaluated after Ni-NP exposure, every experimental group showed a significant increase by up to 76% compared to the control group (0 mg metal/kg body weight: 312 ± 15 ng-at O/min g tissue, $p < 0.01$). Regarding O_2 consumption in the presence of KCN, 0.05 to 1.0 mg metal/kg body weight mice groups were significantly increased compared with the control group (0 mg metal/kg body weight: 96 ± 12 ng-at O/min g tissue, $p < 0.01$) (Fig. 3D). After Fe-NP instillation, a significant increase in total lung O_2 consumption by 48% and 52% was observed at 0.10 and 1.0 mg metal/kg body weight, respectively, compared to the control group (0 mg metal/kg body weight: 284 ± 13 ng-at O/min g tissue, $p < 0.05$). Non-mitochondrial O_2 consumption was also significantly increased by up to 69% compared to the control group (0 mg metal/kg body weight: 137 ± 10 ng-at O/min g tissue, $p < 0.05$) (Fig. 3E).

3.4. Lucigenin chemiluminescence for superoxide and superoxide-products

In our previous findings (Magnani et al., 2013), we have reported that, besides mitochondrial respiration, NOX enzymes also comprise a relevant source of O_2 uptake in lung following environmental PM exposure. Additionally, the activity of this enzyme leads to the production of reactive O_2 species. Production of *superoxide and superoxide-products* were evaluated through the measurement of NADPH-dependent $O_2^{\bullet-}$ production by a chemiluminescence assay, in lung homogenates obtained from mice exposed to increasing doses of metal-coated NP.

Neither Cd-NP nor Cr-NP-exposed animals showed changes in lucigenin chemiluminescence (Fig. 4A and B). Compared to the control group (0 mg metal/kg body weight: 0.82 ± 0.02 AU/min mg protein, $O_2^{\bullet-}$ production after Ni-NP exposure was significantly increased by up to 43% regardless the used dose ($p < 0.01$) (Fig. 4C). After Fe-NP instillation, $O_2^{\bullet-}$ production remained unchanged in the 0.01 mg metal/kg body weight group, but increased by 27% ($p < 0.01$) and 37% ($p < 0.01$) in 0.05 and 0.10 mg metal/kg body weight animals, respectively. At 1.0 mg metal/kg body weight, mice exposed to Fe-NP presented the highest percentage of increase compared with the control group (88%, $p < 0.001$) (Fig. 4D).

3.5. Lung TBARS content

Increased production of reactive O_2 species is able to generate oxidative damage to macromolecules, such as phospholipids. Oxidative damage to lipids was evaluated by the TBARS content of lung homogenates after metal-coated NP treatment at increasing doses.

No differences were observed in mice exposed to Cd-NP when compared to the control group (Fig. 5A). Significant increases in lung TBARS content were found following Cr-NP exposure at 0.05

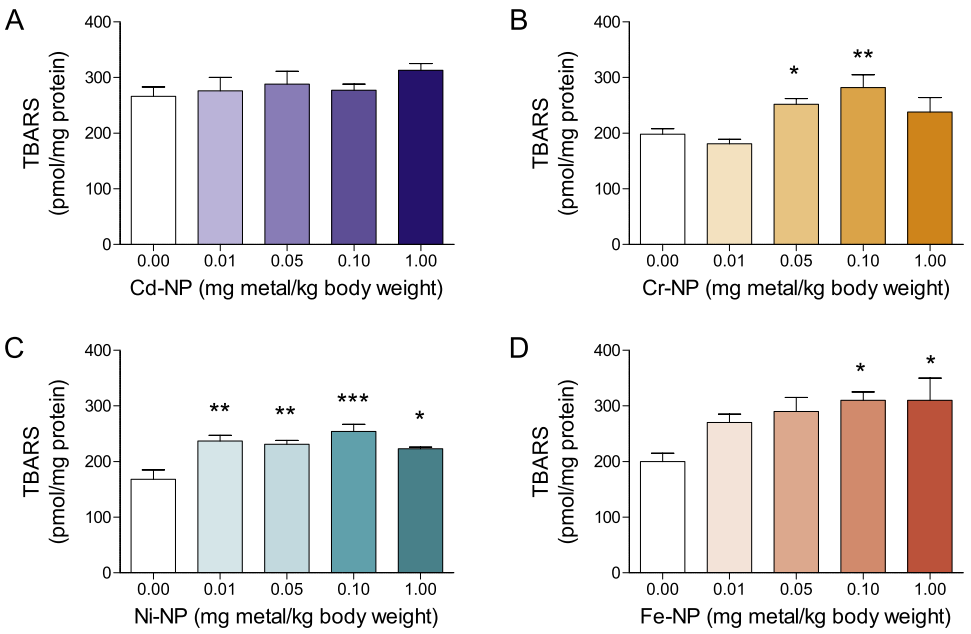

Fig. 5. Lung oxidative damage to phospholipids after the exposure to metal-coated NPs. TBARS content was evaluated by a fluorometric assay in lung homogenates from mice exposed to increasing doses of A) Cd-NP, B) Cr-NP, C) Ni-NP, or D) Fe-NP. $^{*}p < 0.05$, $^{**}p < 0.01$, and $^{***}p < 0.001$ vs. the corresponding control group for each metal (0 mg metal/kg body weight).

and 0.10 mg/kg body weight, by 27% ($p < 0.05$) and 42% ($p < 0.01$), respectively, compared to the control group (0 mg metal/kg body weight: 200 ± 10 pmol/mg protein) (Fig. 5B). Mice exposed to every NP-Ni dose showed a significant increase in TBARS content by up to 51% ($p < 0.05$) (Fig. 5C), as for the two higher Fe-NP doses (0.10 mg metal/kg body weight: 55%, $p < 0.05$; 1.0 mg metal/kg body weight: 55%, $p < 0.05$), when compared to their matched control groups (Fig. 5D).

3.6. Reduced (GSH) and oxidized (GSSG) glutathione levels

GSH is a low molecular weight antioxidant which is readily oxidized to GSSG in order to detoxify a wide variety of oxidant species. A decrease in the GSH/GSSG ratio indicates a shift towards a more oxidized environment, which suggests the occurrence of oxidative stress. Therefore, the GSH/GSSG ratio is one of the most widely used parameters of redox status in cells and tissues (Franco et al., 2007). As it is shown in Table 2, no differences were observed in lung GSH content in any experimental condition in comparison with the control group (0 mg metal/kg body weight: 280 ± 10 μg/g tissue). However, exposure to Cr-NP, Ni-NP, and Fe-NP at 1.0 mg metal/kg body weight leaded to a significant increase in lung GSSG content by 50% ($p < 0.01$), 20% ($p < 0.05$), and 165% ($p < 0.001$), respectively, compared to the control (0 mg metal/kg body weight: 20 ± 2 μg/g tissue). Consequently, GSH/GSSG ratio was decreased in these groups, indicating the occurrence of lung oxidative stress following Cr-NP, Ni-NP, and Fe-NP exposure.

4. Discussion

Numerous epidemiological studies have shown that the exposure to environmental PM positively correlates with increased morbidity and mortality rates (Anderson et al., 2012; Brunekreef and Holgate, 2002; Pope et al., 2002). We and others have previously reported that PM exposure induces lung and systemic inflammation and oxidative stress (Magnani et al., 2011; Marchini et al., 2014; Nurkiewicz et al., 2006), as well as adverse cardiovascular effects (Farraj et al., 2009; Marchini et al., 2013). PM is a heterogeneous mixture that varies in particle size and chemical composition. An increasing body of evidence indicates that rather than the total mass of inhaled particles, PM chemical composition may better correlate with the health outcomes due to the exposure to road traffic emissions (Burnett et al., 2000; Li et al., 2004). In this study, we provide evidence on the differential role of transition metals frequently found in PM and the adverse effects observed in lung after metal-coated NP exposure.

The rationale behind the study was to build NPs resembling particles coated with environmentally relevant transition metals. Cd, Cr, Ni, and Fe were selected, as these metals are among the most frequently found in highly polluted environments, and have been shown to be associated with PM adverse health effects (Dunea et al., 2016; Van Den Heuvel et al., 2016). The construction of NP was carried out following the physical characteristics of particles in environmental pollution (Nel et al., 2006). As shown in Table 1, metal-coated NP size range between 0.17 to 0.70 μm, sharing a similar aerodynamic diameter with fine PM. Moreover, the ultrastructure analysis by TEM revealed that its spherical shape agrees with that shown in previous studies with PM samples (Fischer et al., 1983). NPs were synthesized by the Stöber method, a simple technique that allows uniformity of size and shape of the particles (Foglia et al., 2011). It has previously been shown that this type of NP does no induce relevant toxicity (Kunzman et al., 2011). When NP were evaluated in our model, by comparing lung O_2 consumption in tissue samples obtained after empty silica NP delivery with values obtained after instillation of saline solution, no differences were found among both groups. These results not only confirm that empty silica NP do not modulate lung O_2 metabolism in the present model of acute exposure, but is consistent with the hypothesis that the adverse effects of PM inhalation are mainly due to compounds adsorbed to their surface and not to the presence of the particles *per se*.

Clinical evidence shows that chronic exposure, even at lower doses of PM, has an impact over cardiovascular mortality (Pope, 2004). However, epidemiological studies have also shown that the

Table 2
Lung GSH and GSSG levels after the exposure to metal-coated NPs. GSH and GSSG content was evaluated by HPLC in lung homogenates from mice exposed to increasing doses of metal-coated NPs.

	Dose (mg metal/kg body weight)	GSH (μg/g tissue)	GSSG (μg/g tissue)	GSH/GSSG
Cd-NP	0.00	280 ± 10	20 ± 2	14.0
	0.01	270 ± 40	21 ± 3	12.5
	0.05	260 ± 10	14 ± 2	18.5
	0.10	310 ± 30	19 ± 4	16.3
	1.00	330 ± 30	20 ± 4	16.5
Cr-NP	0.01	250 ± 10	15 ± 1	16.7
	0.05	310 ± 10	20 ± 3	15.5
	0.10	310 ± 10	20 ± 1	15.5
	1.00	270 ± 10	30 ± 3**	9.0
Ni-NP	0.01	260 ± 10	20 ± 4	13.0
	0.05	270 ± 10	18 ± 1	15.0
	0.10	280 ± 10	18 ± 2	15.6
	1.00	280 ± 20	24 ± 1*	11.7
Fe-NP	0.01	305 ± 10	26 ± 4	11.7
	0.05	330 ± 20	24 ± 1	13.8
	0.10	250 ± 10	25 ± 2	10.0
	1.00	250 ± 30	53 ± 1***	4.7

* $p < 0.05$ vs. control group (0 mg metal/kg body weight).
** $p < 0.01$ vs. control group (0 mg metal/kg body weight).
*** $p < 0.001$ vs. control group (0 mg metal/kg body weight).

exposure to high concentrations of PM widely occur in a localized and timely limited manner in many areas of industrialized countries (Brook, 2008). Such exposure to highly concentrated PM environments is known to increase morbidity and mortality within a few hours (Shi et al., 2016). In the present work, we aimed to simulate short-term exposure to PM to investigate the role of transition metals in adverse health effects. The dose range administrated was selected taking into account metal concentrations found in the atmosphere (Valko et al., 2006), and doses used in previous studies (Chen and Lippmann, 2009).

It is accepted that the exposure to air pollution PM triggers an inflammatory response within the lung, as well as endothelial activation and oxidative stress (Kelly and Fussell, 2015). In this scenario, the analysis of lung O_2 metabolism appears to be an important area of study in order to understand the mechanisms of free radicals production, which may lead to the onset and aggravation of respiratory diseases. Lung O_2 consumption was found to be significantly increased after the exposure to most doses of Ni-NP and Fe-NP, and the 0.05 mg metal/kg body weight dose of Cr-NP, while no changes were observed for Cd-NP. Several mechanisms have been suggested to explain this observation, such as increased enzymatic activities and changes in mitochondrial respiration (Vanasco et al., 2008). In order to deeply analyze O_2 consumption after the exposure to metal-coated NPs, KCN was used to evaluate the contribution of non-mitochondrial sources to lung O_2 consumption. These measurements showed the same pattern as the one described for total O_2 consumption, indicating that metal-coated NPs might induce the activities of O_2 consuming enzymes. NOX is of particular interest, as an important non-mitochondrial source of reactive O_2 species elicited by airway inflammation (Van der Vliet, 2011). It has been shown that environmental particles, when internalized by phagocytosis after inhalation, trigger an increased alveolar macrophage count (Becker et al., 2002). In our previous studies, we have shown that the increased $O_2^{\bullet-}$ production triggered by PM exposure was mainly due to increased Nox activity, since inhibition of the enzyme prevented the increased chemiluminescence (Magnani et al., 2011, 2013). In the present model, only Ni-NP and Fe-NP showed the ability to induce a significant increase in $O_2^{\bullet-}$ production. Considering that Nox-dependent $O_2^{\bullet-}$ production is another source of O_2 uptake, the increased enzyme activity may explain, at least in part, the registered increase in lung O_2 consumption.

Oxidative stress is hypothesized to be one of the main mechanisms underlying the adverse health effects associated with the exposure to ambient PM (Kelly, 2003). In order to establish the possible occurrence of pulmonary oxidative stress, TBARS levels were determined as an indicator of oxidative damage, together with the GSH/GSSG ratio as a marker of redox status. The obtained results indicate that the higher doses of Ni-NP and Fe-NP were able to induce an oxidative stress condition, as changes in both the TBARS level and the GSH/GSSG ratio were observed.

Ni and Fe might be more relevant in the health effects associated to short term PM exposure. Both chemical species were able to induce changes in the oxidative metabolism in the lung. The increase in O_2 consumption might be explained by the activation of an inflammatory response, as indicated by the increased NOX activity. Ni was able to induce changes even at low concentrations. This might be explained by the fact that the lung is the main organ where Ni accumulates and exerts its toxic effects. It has been reported that, regardless of the route of administration, concentrations of cytosolic Ni(II) are higher than in other organs (Denkhaus and Salnikow, 2002). The generation of reactive O_2 species at the particle surface via Fenton reaction (Fig. 2) cannot be ruled out as a mechanism that may contribute to the observed oxidative damage, as well as to the occurrence of oxidative stress. Exposure to Cr-NP presented a significant increase only at 0.05 mg metal/kg body weight. Such biphasic responses have also been observed in cell damage mechanisms driven by oxidative stress produced by Cr (Travacio et al., 2001).

Taken together, the present results show different effects for every tested metal. These findings emphasize the importance of transition metals present air PM in adverse health effects, and contribute to the understanding of the pathological mechanisms triggered by the exposure to environmental PM.

Acknowledgments

This study was supported by grants from the Universidad de Buenos Aires (20020130100614BA), Agencia Nacional de Promoción Científica y Tecnológica (PICT-2013-3227), and

Consejo Nacional de Investigaciones Científicas y Técnicas (PIP11220120100321).

References

Analitis, A., Katsouyanni, K., Dimakopoulou, K., Samoli, E., Nikoloulopoulos, A.K., Petasakis, Y., Touloumi, G., Schwartz, J., Anderson, H.R., Cambra, K., Forastiere, F., Zmirou, D., Vonk, J.M., Clancy, L., Kriz, B., Bobvos, J., Pekkanen, J., 2006. Short-term effects of ambient particles on cardiovascular and respiratory mortality. Epidemiology 17, 230–233.

Anderson, J.O., Thundiyil, J.G., Stolbach, A., 2012. Clearing the air: a review of the effects of particulate matter air pollution on human health. J. Med. Toxicol. 8, 166–175.

Arantes-Costa, F., Lopes, F., Toledo, A., Magliarelli-Filho, P., Moriya, H., Carvalho-Oliveira, R., Mauad, T., Saldiva, P., Martins, M., 2008. Effects of Residual Oil Fly Ash (ROFA) in mice with chronic allergic pulmonary inflammation. Toxicol. Pathol. 36, 680–686.

Becker, S., Soukup, J.M., Gallagher, J.E., 2002. Differential particulate air pollution induced oxidant stress in human granulocytes, monocytes and alveolar macrophages. Toxicol. In Vitro 16, 209–218.

Brook, R.D., Franklin, B., Cascio, W., Hong, Y., Howard, G., Lipsett, M., Luepker, R., Mittleman, M., Samet, J., Smith Jr., S.C., Tager, I., 2004. Air pollution and cardiovascular disease: a statement for healthcare professionals from the Expert Panel on Population and Prevention Science of the American Heart Association. Circulation 109 (21), 2655–2671.

Brook, R.D., 2008. Cardiovascular effects of air pollution. Clin. Sci. (Lond.) 115, 175–187.

Brunekreef, B., Holgate, S.T., 2002. Air pollution and health. Lancet 360, 1233.

Burnett, R.T., Brook, J., Dann, T., Delocla, C., Philips, O., Cakmak, S., Vincent, R., Goldberg, M.S., Krewski, D., 2000. Association between particulate- and gas-phase components of urban air pollution and daily mortality in eight Canadian cities. Inhal. Toxicol. 12 (Suppl 4), S15–S39.

Chen, L.C., Lippmann, M., 2009. Effects of metals within ambient air particulate matter (PM) on human health. Inhal. Toxicol. 21, 1–31.

Chen, Q., Vazquez, E.J., Moghaddas, S., Hoppel, C.L., Lesnefsky, E.J., 2003. Production of reactive oxygen species by mitochondria: central role of complex III. J. Biol. Chem. 278, 36027–36031.

Copello, G.J., Varela, F., Vivot, R.M., Díaz, L.E., 2007. Immobilized chitosan as biosorbent for the removal of Cd(II), Cr(III) and Cr(VI) from aqueous solutions. Bioresour. Technol. 99 (14), 6538–6544.

Delfino, R.J., Sioutas, C., Malik, S., 2005. Potential role of ultrafine particles in associations between airborne particle mass and cardiovascular health. Environ. Health Perspect. 113 (8), 934–946.

Denkhaus, E., Salnikow, K., 2002. Nickel essentiality, toxicity and carcinogenicity. Crit. Rev. Oncol. 42, 35–56.

Dominici, F., Peng, R.D., Bell, M.L., Pham, L., McDermott, A., Zeger, S.L., Samet, J.M., 2006. Fine particulate air pollution and hospital admission for cardiovascular and respiratory diseases. JAMA 295, 1127–1134.

Dunea, D., Iordache, S., Liu, H.Y., Bøhler, T., Pohoata, A., Radulescu, C., 2016. Quantifying the impact of PM2. 5 and associated heavy metals on respiratory health of children near metallurgical facilities. Environ. Sci. Pollut. Res. Int. 23 (15), 15395–15406.

Evelson, P., Travacio, M., Repetto, M., Escobar, J., Llesuy, S., Lissi, E., 2001. Evaluation of total reactive antioxidant potential (TRAP) of tissue homogenates and their cytosols. Arch. Biochem. Biophys. 388, 261–266.

Farraj, A.K., Haykal-Coates, N., Winsett, D.W., Hazari, M.S., Carll, A.P., Rowan, W.H., Ledbetter, A.D., Cascio, W.E., Costa, D.L., 2009. Increased non-conducted P-wave arrhythmias after a single oil fly ash inhalation exposure in hypertensive rats. Environ. Health Perspect. 117 (5), 709–715.

Fischer, G.L., McNeill, K.L., Prentice, B.A., McFarlandt, A.R., 1983. Physical and biological studies of coal and oil fly ash. Environ. Health Perspect. 51, 181–186.

Foglia, M.L., Alvarez, G.S., Catalano, P.N., Mebert, A.M., Diaz, L.E., Coradin, T., Desimone, M.F., 2011. Recent patents on the synthesis and application of silica nanoparticles for drug delivery. Recent Pat. Biotechnol. 5, 54–61.

Franco, R., Schoneveld, O.J., Pappa, A., Panayiotidis, M., 2007. The central role of glutathione in the pathophysiology of human diseases. Arch. Physiol. Biochem. 113, 234–258.

Goldsmith, C.A., Imrich, A., Danaee, H., Ning, Y.Y., Kobzik, L., 1998. Analysis of air pollution particulate-mediated oxidant stress in alveolar macrophages. J. Toxicol. Environ. Health A 54, 529–545.

Kelly, F., Fussell, J., 2015. Linking ambient particulate matter pollution effects with oxidative biology and immune responses. Ann. N.Y. Acad. Sci. 1340, 84–94.

Kelly, F.J., 2003. Oxidative stress: its role in air pollution and adverse health effects. Occup. Environ. Med. 60, 612–616.

Kunzman, A., Andersson, B., Vogt, C., Feliu, N., Ye, F., Gabrielsson, S., Toprak, M., Buerki-Thurnherr, T., Laurent, S., Vahter, M., Krug, H., Muhammed, M., Sheynius, A., Fadeel, B., 2011. Efficient internalization of silica-coated iron oxide nanoparticles of different size by primary human macrophages and dendritic cells. Toxicol. Appl. Pharmacol. 253, 81–93.

Leonard, S.S., Harris, G.K., Shi, X., 2004. Metal-induced oxidative stress and signal transduction. Free Radic. Biol. Med. 37, 1921–1942.

Li, N., Nel, A.E., 2008. The role of oxidative stress in ambient particulate matter-induced lung diseases and its implications in the toxicity of engineered nanoparticles. Free Radic. Biol. Med. 44 (9), 1689–1699.

Li, N., Alam, J., Venkatesan, M.I., Eiguren-Fernandez, A., Schmitz, D., Di Stefano, E., Slaughter, N., Killeen, E., Wang, X., Huang, A., Wang, M., Miguel, A.H., Cho, A., Sioutas, C., Nel, A.E., 2004. Nrf2 is a key transcription factor that regulates antioxidant defense in macrophages and epithelial cells: protecting against the proinflammatory and oxidizing effects of diesel exhaust chemicals. J. Immunol. 173 (5), 3467–3481.

Lowry, O., Rosebrough, A., Farr, A., Randall, R., 1951. Protein measurement with the phenol reagent. J. Biol. Chem. 193, 265–275.

Magnani, N., Marchini, T., Tasat, D., Alvarez, S., Evelson, P., 2011. Lung oxidative metabolism after exposure to ambient particles. Biochem. Biophys. Res. Commun. 412, 667–672.

Magnani, N., Marchini, T., Vanasco, V., Tasat, D., Alvarez, S., Evelson, P., 2013. Reactive oxygen species produced by NADPH oxidase and mitochondrial dysfunction in lung after an acute exposure to Residual Oil Fly Ashes. Toxicol. Appl. Pharmacol. 270, 31–38.

Marchini, T., Magnani, N., D'Annunzio, V., Tasat, D., Gelpi, R.J., Alvarez, S., Evelson, P., 2013. Impaired cardiac mitochondrial function and contractile reserve following an acute exposure to environmental particulate matter. Biochim. Biophys. Acta 1830, 2545–2552.

Marchini, T., Magnani, N.D., Paz, M.L., Vanasco, V., Tasat, D., González Maglio, D.H., Alvarez, S., Evelson, P., 2014. Time course of systemic oxidative stress and inflammatory response induced by an acute exposure to Residual Oil Fly Ash. Toxicol. Appl. Pharmacol. 274, 274–282.

Nel, A., Xia, T., Madler, L., Li, N., 2006. Toxic potential of materials at the nanolevels. Science 311, 622–627.

Nel, A., 2005. Atmosphere: air pollution-related illness: effects of particles. Science 308, 804–806.

Nurkiewicz, T.R., Porter, D.W., Barger, M., Millecchia, L., Rao, K.M., Marvar, P.J., Hubbs, A.F., Castranova, V., Boegehold, M.A., 2006. Systemic microvascular dysfunction and inflammation after pulmonary particulate matter exposure. Environ. Health Perspect. 114 (3), 412–419.

Poderoso, J., Fernandez, S., Carreras, M.C., Tchercanski, D., Acevedo, C., Rubio, M., Peralta, J., Boveris, A., 1994. Liver oxygen uptake dependence and mitochondrial function in septic rats. Circ. Shock 44, 175–182.

Pope, C.A., Burnett, R., Thun, M., 2002. Lung cancer, cardiopulmonary mortality and long-term exposure to fine particulate air pollution. J. Am. Med. Assoc. 287, 1132–1141.

Pope, C.A., 2004. Air pollution and health – good news and bad. N. Engl. J. Med. 351 (11), 1132–1134.

Rodriguez-Ariza, A., Toribio, F., López-Barea, J., 1994. Rapid determination of glutathione status in fish liver using high-performance liquid chromatography and electrochemical detection. J. Chromatogr. Biomed. Appl. 656, 311–318.

Shi, L., Zanobetti, A., Kloog, I., Coull, B.A., Koutrakis, P., Melly, S.J., Schwartz, J.D., 2016. Low-concentration PM2.5 and mortality: estimating acute and chronic effects in a population-based study. Environ. Health Perspect. 124 (1), 46–52.

Southam, D.S., Dolovich, M., O'Byrne, P.M., Inman, M.D., 2002. Distribution of intranasal instillations in mice: effects of volume, time, body position, and anaesthesia. Am. J. Physiol. Lung Cell Mol. Physiol. 282, 833–839.

Stöber, W., Fink, A., 1968. Controlled growth of monodisperse silica spheres in the micron size range. J. Colloid Interface Sci. 26 (1), 62–69.

Thomassen, L.C., Aerts, A., Rabolli, V., Lison, D., Gonzalez, L., Kirsch-Volders, M., Napierska, D., Hoet, P.H., Kirschhock, C.E., Martens, J.A., 2010. Synthesis and characterization of stable monodisperse silica nanoparticle sols for *in vitro* cytotoxicity testing. Langmuir 26 (1), 328–335.

Travacio, M., Polo, J.M., Llesuy, S., 2001. Chromium (VI) induces oxidative stress in the mouse brain. Toxicology 162 (2), 139–148.

Valdez, L.B., Zaobornyj, T., Bombicino, S., Iglesias, D.E., Boveris, A., Donato, M., D'Annunzio, V., Buchholz, B., Gelpi, R.J., 2011. Complex I syndrome in myocardial stunning and the effect of adenosine. Free Radic. Biol. Med. 15, 1203–1212.

Valko, M., Rhodes, C.J., Moncol, J., Izakovic, M., Mazur, M., 2006. Free radical, metals and antioxidants in oxidative stress-induced cancer. Chem. Biol. Interact. 160, 1–40.

Van Den Heuvel, R., Den Hond, E., Govarts, E., Colles, A., Koppen, G., Staelens, J., Mampaey, M., Janssen, N., Schoeters, G., 2016. Identification of PM_{10} characteristics involved in cellular responses in human bronchial epithelial cells (Beas-2B). Environ. Res. 149, 48–56.

Van der Vliet, A., 2011. Nox enzymes in allergic airway inflammation. Biochim. Biophys. Acta 1810, 1035–1044.

Vanasco, V., Cimolai, M.C., Evelson, P., Alvarez, S., 2008. The oxidative stress and the mitochondrial dysfunction caused by endotoxemia are prevented by α-lipoic acid. Free Radic. Res. 42, 815–823.

Vaquero, E.C., Edderkaoui, M., Pandol, S.J., Gukovsky, I., Gukovskaya, A.S., 2004. Reactive oxygen species produced by NAD(P)H oxidase Inhibit apoptosis in pancreatic cancer cells. J. Biol. Chem. 279, 34643–34654.

Yagi, K., 1976. A simple fluorometric assay lipoperoxide in blood plasma. Biochem. Med. 15, 212–216.